Potency of bisresorcinol from *Heliciopsis terminalis* on skin aging: in vitro bioactivities and molecular interactions

Charinrat Saechan [1], Uyen Hoang Nguyen [2], Zhichao Wang [2], Sachiko Sugimoto [2], Yoshi Yamano [2], Katsuyoshi Matsunami [2], Hideaki Otsuka [3], Phan Minh Giang [4], Pham Hung Viet [5], Varomyalin Tipmanee [Corresp., 6], Jasadee Kaewsrichan [Corresp. 1]

[1] Department of Pharmaceutical Chemistry and Drug Delivery System Excellence Center, Faculty of Pharmaceutical Sciences, Prince of Songkla University, Songkhla, Thailand

[2] Graduate School of Biomedical and Health Sciences, Hiroshima University, Hiroshima, Japan

[3] Faculty of Pharmacy, Yasuda Women's University, Hiroshima, Japan

[4] Faculty of Chemistry, VNU University of Science,, Vietnam National University, Hanoi, Vietnam

[5] Research Center for Environmental Technology and Sustainable Development, VNU University of Science, Vietnam National University, Hanoi, Vietnam

[6] Department of Biomedical Sciences and Biomedical Engineering, Faculty of Medicine, Prince of Songkla University, Songkhla, Thailand

Corresponding Authors: Varomyalin Tipmanee, Jasadee Kaewsrichan
Email address: tvaromya@medicine.psu.ac.th, jasadee.k@psu.ac.th

Background: A bisresorcinol was isolated as the main constituent of *Heliciopsis terminalis*'s trunk (Proteaceae). Recently, resorcinol is applied as an active whitening agent in various cosmetic products. Because of the structural mimic to resorcinol, benefits of the bisresorcinol as an aging-enzyme antagonist were demonstrated in this study.

Methods: The bisresorcinol was purified from the crude ethanolic extract of *H. terminalis*'s trunk by solvent extraction and preparative chromatography, respectively. Inhibitory activity on collagenase, elastase, and tyrosinase of the compound was investigated by using a different spectroscopic technique. Molecular docking was carried out to predict possible interactions of the substance around the enzyme active sites.

Results: The IC_{50} values on collagenase of the bisresorcinol and caffeic acid were 156.7±0.7 and 308.9±1.6 µmole L^{-1}, respectively. For elastase activity, the IC_{50} of 33.2±0.5 and 34.3±0.3 µmole L^{-1} was respectively determined for the bisresorcinol and ursolic acid. The bisresorcinol was inhibitory to tyrosinase by exhibiting the IC_{50} of 22.8 µmole L^{-1}, and that of 78.4 µmole L^{-1} was present for β-arbutin. The bisresorcinol bound to collagenase, elastase, and tyrosinase with the respective binding energies of -5.89, -5.69, and -6.57 kcal mol^{-1}. These binding energies were in the same ranges of tested inhibitors. The aromatic phenol groups in the structure were responsible for principle as well as supporting binding interactions with enzymes. Hydrogen binding due to hydroxyl groups and π -related attractive forces from an aromatic ring(s) provided binding versatility to bisresorcinol.

Conclusion: The bisresorcinol purified from *H. terminalis* might be useful for inclusion in cosmetic products as an aging-enzyme antagonist.

1 **Potency of bisresorcinol from *Heliciopsis terminalis* on skin aging: *in vitro* bioactivities and**

2 **molecular interactions**

3 Charinrat Saechan[1], Uyen Hoang Nguyen[2], Zhichao Wang[2], Sachiko Sugimoto[2], Yoshi

4 Yamano[2], Katsuyoshi Matsunami[2], Hideaki Otsuka[3], Phan Minh Giang[4], Pham Hung Viet[5],

5 Varomyalin Tipmanee[6], and Jasadee Kaewsrichan[1]

6 [1]Department of Pharmaceutical Chemistry and Drug Delivery System Excellence Center, Faculty

7 of Pharmaceutical Sciences, Prince of Songkla University, Hat-Yai, Songkhla, Thailand

8 [2]Graduate School of Biomedical and Health Sciences, Hiroshima University, 1-2-3 Kasumi,

9 Minami-ku, Hiroshima, Japan

10 [3]Faculty of Pharmacy, Yasuda Women's University, 6-13-1 Yasuhigashi, Asaminami-ku,

11 Hiroshima, Japan

12 [4]Faculty of Chemistry, VNU University of Science, Vietnam National University; 19 Le Thanh

13 Tong, Hanoi, Vietnam

14 [5]Research Center for Environmental Technology and Sustainable Development, VNU University

15 of Science, Vietnam National University, Hanoi, 334 Nguyen Trai Street, Hanoi, Vietnam

16 [6]Department of Biomedical Sciences and Biomedical Engineering, Faculty of Medicine, Prince

17 of Songkla University, Hat-Yai, Songkhla, Thailand

19 **Corresponding Authors:**

20 Jasadee Kaewsrichan, Department of Pharmaceutical Chemistry, Faculty of Pharmaceutical

21 Sciences, Prince of Songkla University, Hat-Yai, Songkhla, 90112, Thailand

22 E-mail address: jasadee.k@psu.ac.th

23   Varomyalin Tipmanee, Department of Biomedical Sciences and Biomedical Engineering,

24   Faculty of Medicine, Prince of Songkla University, Hat-Yai, Songkhla, 90112, Thailand

25   Email address: tvaromya@medicine.psu.ac.th

26   **Abstract**

27   **Background:** A bisresorcinol was isolated as the main constituent of *Heliciopsis terminalis*'s

28   trunk (Proteaceae). Recently, resorcinol is applied as an active whitening agent in various

29   cosmetic products. Because of the structural mimic to resorcinol, benefits of the bisresorcinol as

30   an aging-enzyme antagonist were demonstrated in this study.

31   **Methods:** The bisresorcinol was purified from the crude ethanolic extract of *H. terminalis*'s

32   trunk by solvent extraction and preparative chromatography, respectively. Inhibitory activity on

33   collagenase, elastase, and tyrosinase of the compound was investigated by using a different

34   spectroscopic technique. Molecular docking was carried out to predict possible interactions of

35   the substance around the enzyme active sites.

36   **Results:** The IC_{50} values on collagenase of the bisresorcinol and caffeic acid were 156.7±2.3 and

37   308.9±13.7 µmol L^{-1}, respectively. For elastase activity, the IC_{50} of 33.2±1.1 and 34.3±0.6 µmol

38   L^{-1} was respectively determined for the bisresorcinol and ursolic acid.

39   The bisresorcinol was inhibitory to tyrosinase by exhibiting the IC_{50} of 22.6 µmol L^{-1}, and that

40   of 78.5 µmol L^{-1} was present for β-arbutin. The bisresorcinol bound to collagenase, elastase, and

41   tyrosinase with the respective binding energies of -5.89, -5.69, and -6.57 kcal mol^{-1}. These

42   binding energies were in the same ranges of tested inhibitors. The aromatic phenol groups in the

43   structure were responsible for principle as well as supporting binding interactions with enzymes.

44   Hydrogen binding due to hydroxyl groups and π -related attractive forces from an aromatic

45   ring(s) provided binding versatility to bisresorcinol.

46   **Conclusion:** The bisresorcinol purified from *H. terminalis* might be useful for inclusion in

47   cosmetic products as an aging-enzyme antagonist.

48   **Introduction**

49   A bisresorcinol, (8'Z)-3,5-dihydroxy-1-[16'-(3",5"-dihydroxyphenyl)-8'-hexadecen-1'-yl]benzene,

50   has been isolated as an abundant constituent from the trunk of *Heliciopsis terminalis* (Kurz)

51   Sleumer, which is a plant of Proteaceae family and has been used by ethnic people in Vietnam

52   for hepatoprotective effect. To date, medical benefits of this compound as an agent for anti-

53   inflammation, inhibition of malondialdehyde (MDA) production, and hepatoprotection, have

54   been clarified *in vitro* and *in vivo* (Giang *et al.,* 2019). It is apparent in that a molecule of the

55   bisresorcinol contains two resorcinol molecules (EC No 203-585-2), bonded together with *meta-*

56   $C_7H_{14}C=CC_7H_{14}$ linkage (Fig. 1a). Resorcinol is recently applied in a form of facial concentrated

57   serum for white therapy. Based on the Scientific Committee on Consumer Safety (SCCS

58   1270/09, European Commission, 2010), resorcinol has been regulated as an oxidant in products

59   intended for coloring eyelashes at concentration ranges up to 1.25%, or in hair lotions and

60   shampoos at concentration ranges up to 0.5%. Cosmetical applications of resorcinol are thus

61   diverse. For whitening agents, inhibition of melanin synthesis by melanocytes that reside in the

62   basal cell layer of epidermis has been assumed. Tyrosinase (EC 1.14.18.1) is a key enzyme for

63   catalyzing melanogenesis in which L-tyrosine is used as the substrate. Although melanin helps

64   protect skin form damage of UV rays, excess melanin production can cause hyperpigmentation,

65   freckle, and age spot. In addition to resorcinol, various synthetic and natural compounds with

66   distinct chemical structures have been demonstrated to exhibit anti-tyrosinase activity (Dobos *et*

67   *al.,* 2015).

68 UV radiation is a major external factor that causes skin aging. Instead, skins can age over

69 time by reactive oxygen species (ROS) and lipid peroxides that are internally produced after UV

70 exposure. Secondary products from lipid peroxide metabolisms can damage elastin and collagen

71 fibers of extracellular matrices (ECMs). Therefore, exposure to UV rays can result in

72 dehydration, loss of elasticity, as well as wrinkles of the skins. To our knowledge, the ECMs are

73 periodically remodeled to maintain normal tissue structures in accompany with that expired

74 tissue proteins are properly degraded by matrix metalloproteinases, such as collagenases, and

75 serine proteases like elastases (Thring, Hili & Naughton, 2009). In addition, both quantities and

76 activities of aging enzymes have been increased by oxidative stress, leading to extensive ECMs

77 degradation and progressive aging (Sherratt *et al.,* 2019). Therefore, compounds that can form

78 complexes with metal ions are anticipated to be inhibitory to collagenases, elastases, and

79 tyrosinase accordingly (Selvaraj et al., 2014). This project aims to determine biological effects of

80 the bisresorcinol on tyrosinase, collagenase, and elastase *in vitro*, and docking technique was

81 carried out to clarify their interactions at molecular levels. It is hopeful to delay the aging process

82 and improve skin appearance by the bisresorcinol.

83

84 **Materials & Methods**

85 **Chemicals and Instruments**

86 All the chemicals used in this study were of analytical grade. Organic solvents, including 1-

87 butanol, acetone, chloroform (also for NMR), and ethyl acetate, were purchased from KANTO

88 CHEMICAL CO., INC., Japan. Chemicals, such as hydrochloric acid, K_2HPO_4, KH_2PO_4, L-

89 tyrosine, silica gel, octadecyl silica gel, and tris (hydroxymethyl) aminomethane, were bought

90 from NACALAI TESQUE, INC., Japan. Standard substances, including β-arbutin, caffeic acid,

91   and ursolic acid, and tricine were obtained from Tokyo Chemical Industry, Japan. Enzymes, such

92   as collagenase, elastase, and tyrosinase, including N-succinyl-Ala-Ala-Ala-p-nitroanilide

93   (SANA) and dimethyl sulfoxide (DMSO), were acquired from Sigma-Aldrich, Germany. DMSO

94   and methanol (NMR grade) were purchased from ISOTEC®, Sigma-Aldrich, Germany. A

95   peptide: MOCAc-PRO-Leu-Gly-Leu-A$_2$pr(Dnp)-Ala-Arg-NH$_2$, was ordered from Peptide

96   Institute, Inc., Japan. Instruments used included HPLC (SCL-10A sp/RID-6A/c-R3A,

97   SHIMADZU), Fluorescence microplate reader (Enspire 2300 Multimode reader, PerkinElmer),

98   HR-ESI-MS (LTQ orbitrap XL, Thermo Fisher Scientific), Infrared Spectrophotometer (FT-720,

99   HORIBA), Nuclear Magnetic Resonance Spectrometer (ECA-500/600, JEOL), and UV-Vis

100 microplate reader (Multiskan Go, Thermo Scientific).

101 **Compound Purification, Identification and Ratification**

102 The crude extract in ethanol of *H. terminalis*'s trunk was generously obtained from Professor

103 P.M. Giang, Faculty of Chemistry, Vietnam National University, Hanoi, Vietnam with voucher

104 specimen number of HNIP-18473. Then, it was partitioned in methanol/n-hexane by 3 times

105 repeated. The methanol layer was evaporated to nearly dry and subsequently partitioned in ethyl

106 acetate/1-butane. The ethyl acetate layer was vaporized until its volume was reduced by 80%.

107 The resulting viscous liquid was then purified on silica gel column using chloroform/methanol

108 gradient elution as follows: 100% chloroform, 30:1, 20:1, 10:1, 7:1, 5:1, 3:1, 3:2, and 2:1 of

109 chloroform/methanol, and 100% methanol, respectively. The eluent from the 5:1 mixed solvent

110 was collected and evaporated to one fourths volume, followed by the separation on the ODS

111 column using gradient elution of methanol and acetone. The desired compound, i.e.,

112 bisresorcinol (Fig. 1), was obtained from eluents containing 70% acetone and confirmed by MS,

113   NMR and IR spectroscopies in regard to the instrumental library data. Thin layer

114   chromatography was used for estimation of its purity.

115   **Biological Activity Assays**

116   *In vitro* experiments that consisted of enzyme-inhibitory assays on collagenase, elastase and

117   tyrosinase for the bisresorcinol and known inhibitors were carried out as follows.

118   **Collagenase inhibition**

119   The recent anti-collagenase assay was modified from that previously described by Widyowati *et*

120   *al.* (2016). In brief, 50 mmol L^{-1} tricine buffer pH 7.5 supplemented with 400 mmol L^{-1} NaCl

121   and 10 mmol L^{-1} CaCl$_2$ was used as the buffering diluent. Collagenase from *Clostridium*

122   *histolyticum* (EC.3.4.24.3) was dissolved in the buffer to a concentration of 1 mg L^{-1}. The

123   enzyme substrate, MOCAc-PRO-Leu-Gly-Leu-A$_2$pr (Dnp)-Ala-Arg-NH$_2$, was prior dissolved in

124   DMSO and subsequently diluted in the buffer to a concentration of 1 mmol L^{-1}. A sample

125   dissolved in DMSO was diluted to different concentrations by using the buffer. A 2-µl sample

126   solution was incubated with 100 µl enzyme solution at 37°C for 10 min. Then, a 50-µl substrate

127   was added and thoroughly mixed. Fluorescence emission (F) at 405 nm was immediately

128   recorded and continually monitored for 30 min using a wavelength of 320 nm for excitation.

129   Caffeic acid was used as a position control (Fig. 1). Negative control was performed with water.

130   The percent inhibition (%) was calculated from the equation below:

131     $$\% \text{ Inhibition} = \{1 - (F_{sam,30} - F_{sam,0}) \div (F_{cont,30} - F_{cont,0})\} \times 100.$$

132   **Elastase Inhibition**

133   The assay according to Abhijit & Manjushree (2010) was applied with some modifications.

134   Briefly, the buffer system was 0.2 mM Tris-HCl buffer (pH 8.0). A solution of 1 µg mL^{-1}

135   porcine pancreatic elastase (EC.3.4.21.36) was prepared in sterile water. The enzyme substrate,

136   N-Succinyl-Ala-Ala-Ala-p-nitroanilide (SANA), was dissolved in the buffer to a concentration

137   of 80 mmol L^{-1}. A sample dissolved in DMSO was diluted to various concentrations by using

138   the buffer. A 100-µl sample solution was mixed with 50 µl enzyme solution and incubated for 15

139   min. After that 50 µl of the enzyme substrate solution was added and thoroughly mixed. The

140   OD_{410} was measured immediately (0 min) and after incubation overnight (o/n) at 37°C by using a

141   microplate reader. Ursolic acid was used as a positive control (Fig. 1), and water was used as a

142   negative control. The percentage inhibition (%) was calculated by the following equation:

143   % Inhibition = $\{1- [(A_{sam,o/n} - A_{sam,0}) \div (A_{cont,o/n} - A_{cont,0})]\} \times 100$.

144   **Tyrosinase Inhibition**

145   The used tyrosinase inhibitory assay was adopted from the previously described method

146   (Jiratchayamaethasakul *et al.,* 2020). In brief, the assay was carried out in 0.05 mol L^{-1}

147   phosphate buffer pH 6.8. Mushroom tyrosinase (EC.1.14.18.1) was dissolved in the buffer to a

148   concentration of 100 units mL^{-1}. L-tyrosine, an enzyme substrate, was prepared to a

149   concentration of 0.25 mg mL^{-1} in the buffer. A test compound dissolved in DMSO was diluted to

150   concentrations ranging between 0.625 and 10 mg mL^{-1}. Into a well of 96-well plates, 10 µl

151   sample and 40 µl L-tyrosine solution were mixed and incubated for 10 min at room temperature.

152   After that 50 µl enzyme solution was inoculated and mixed thoroughly. The reaction was

153   stopped afterward by incubation on ice for 1 min. The OD_{475} was measured using a microplate

154   reader. β-Arbutin and water were used as a positive control (Fig. 1) and a negative counterpart,

155   respectively. The percentage inhibition (%) was calculated by the equation as follows:

156   % Inhibition = $\{1 - (A_{sam,10} - A_{sam,0}) \div (A_{cont,10} - A_{cont,0})\} \times 100$.

157 **Molecular Docking Study**

158 **Preparation of Ligands and Receptors**

159 Three-dimensional (3D) structures of bisresorcinol (CID 8917124) and reference compounds,

160 including substrates and inhibitors, were downloaded from PubChem database for molecular

161 docking study. A ligand structure was prepared in a Protein Data Bank (PDB) format file using

162 Online SMILES Translator and Structure File Generator (https://cactus.nci.nih.gov/translate/).

163 The crystal structures of enzymes, such as collagenase (PDB ID 2Y6I), elastase (PDB ID

164 1BRU), and tyrosinase (PDB ID 2Y9X) were obtained from RCSB protein database

165 (http://www.rcsb.org). The water and the attached molecules were dissected from all selected

166 protein structures. Meanwhile, polar hydrogen atoms were added in the crystallized protein

167 structures by AutoDockTools 1.5.6. Files of target proteins and other used compounds were

168 saved in PDBQT format before performing the molecular docking.

169 **Selection of Active Site Residues and Molecular Docking**

170 Grid and docking protocols of the active site predictions were prepared using AutoDockTools

171 1.5.6. Grid sites were set spacing of 0.375 Å. The x-y-z dimensions were set to be 126-135-160

172 $Å^3$ for collagenase, 130-120-126 $Å^3$ for elastase, and 80-80-80 $Å^3$ for tyrosinase. Grid box

173 centers (with offset values in AutoDockTools) were 31.869 (5.000), -19.41 (-25.000), and 17.815

174 for collagenase, 30.048 (-0.972), 51.253 (-2.722), 17.6 for elastase, and -8.407 (-1.000), -23.795

175 (-0.250), -36.019 (-3.500) for tyrosinase, respectively. The protein structure was used as a rigid

176 entity while the ligand compound was set as a flexible molecule. Docking study was performed

177 using the Lamarckian genetic algorithm (GA) implemented by AutoDock4 version 4.2. The

178 number of GA runs was 50 with a popular size of 200. The binding energy (ΔG_{bind}) was analyzed

179 by ADT. Interaction(s) was visualized using BIOVIA Discovery Studio (BIOVIA, 2020).

180   Molecular interaction between the compound and a protein receptor was analyzed and visualized

181   using BIOVIA Discovery Studio software (BIOVIA, 2020). The structure of protein binding site

182   compound was visualized using Visual Molecular Dynamics (VMD) package (Humphrey, Dalke

183   & Schulten, 1996).

184   **Statistical Analysis**

185   For *in vitro* study, each experiment was done in triplicate. Data were expressed as means ±

186   standard error of the mean (SEM). The Student's t-test was used to evaluate differences between

187   results, and *p*-values of < 0.01 were indicated to be significantly different. The performance

188   regarding statistics was run on Libre Office Calc 5 in Ubuntu 16.04.6 LTS software.

189

190   **Results**

191   A major constituent was successfully purified from *H. terminalis*'s trunk by using solvent

192   extraction and reverse phase HPLC techniques, respectively. The acquired ^{1}H-NMR and ^{13}C-

193   NMR spectra were compared to those of reference substances through the SciFinder

194   (https://scifinder.cas.org/) and found to correspond with (8'Z)-1,3-dihydroxy-5-[16'-(3",5"-

195   dihyroxyphenyl)-8'-hexadecen-1'-yl] benzene (Chaturvedula *et al.,* 2002). It was classified as one

196   of bisresorcinols. This recent bisresorcinol had the molecular formula of $C_{28}H_{40}O_4$ with the

197   molecular weight of 463.2819 Dalton. The extraction yield was calculated to be 0.086%, based

198   on the trunk' dried weight. Its purity was more than 98%, concerning the ^{1}H and ^{13}C-NMR

199   spectra acquired (see Figure S1 and S2).

200   ***In vitro* bioactivity analysis**

201   Antagonistic effects of the bisresorcinol on aging enzymes, such as collagenase, elastase, and

202   tyrosinase were determined *in vitro* by using a distinct spectroscopic method. Results were

203   summarized in Table 1 and Fig. 2. For collagenase inhibition, test samples in a range of 50-550

204   μmol L^{-1} were prepared using MOCAc-PRO-Leu-Gly-Leu-A$_2$pr (Dnp)-Ala-Arg-NH$_2$ as the

205   enzyme substrate and caffeic acid as an enzyme inhibitor. It was indicated that the bisresorcinol

206   at a concentration of 156.7 μmol L^{-1} decreased the enzyme activity by 50% (IC$_{50}$). Instead, the

207   IC$_{50}$ of caffeic acid was 308.9±13.7 μmol L^{-1}. Thus, anti-collagenase activity of the bisresorcinol

208   was significantly stronger than caffeic acid.

209   Inhibition of elastase enzyme was determined at a concentration range between 10 and

210   100 μmol L^{-1}. The residual enzyme activity was spectroscopically measured at 410 nm in

211   response to the amount of *p*-nitroaniline released from the substrate SANA after cleavage. The

212   bisresorcinol strongly inhibited elastase activity in a concentration-dependent manner with the

213   maximum inhibition of 100% at 50 μmol L^{-1}. However, the inhibition decreased rapidly at

214   concentrations less than 30 μmol L^{-1}. Notably, the dose-response curve of ursolic acid was less

215   steep than that of the bisresorcinol by reaching 80% inhibition at 100 μmol L^{-1}. The IC$_{50}$ values

216   of the bisresorcinol and ursolic acid were respectively 33.2 and 34.3 μmol L^{-1}, which were not

217   significantly different.

218   In analysis of tyrosinase inhibition, samples were diluted to a concentration range of 10-

219   100 μmol L^{-1}. L-tyrosine was used as a substrate of mushroom tyrosinase and β-arbutin was a

220   known inhibitor. The bisresorcinol showed the IC$_{50}$ of 22.6 μmol L^{-1}. The IC$_{50}$ of β-arbutin was

221   78.5 μmol L^{-1}. Our test compound showed 100% inhibition at 50 μmol L^{-1}. In contrast, the

222   enzyme inhibition of β-arbutin higher than 50% was not determined in the tested range.

223   **Molecular interaction analysis**

224   Molecular docking was applied to predict binding sites of test compounds to protein receptors,

225   such as collagenase, elastase and tyrosinase, in comparison with known inhibitors of a

226   corresponding enzyme (supplement information). Consisting with previous publications, the

227   relative binding affinity was evaluated meanwhile binding interactions were illustrated through

228   the best predicted conformation (Teajaroen *et al.*, 2020; Jewboonchu *et al.*, 2020;

229   Tanawatsoontorn *et al.*, 2020; Saeloh *et al.*, 2017).

230   For collagenase enzyme, results of ligand-protein interactions were demonstrated in Fig.

231   3 and Table S1 (supplement data). The binding energy of -5.89 kcal mol^{-1} to clostridial

232   collagenase (PDB ID 2Y6I) was presented by the bisresorcinol. A range of the binding energy

233   between -3.68 and -7.90 kcal mol^{-1} was determined for other known collagenase inhibitors,

234   including caffeic acid.

235   Both the bisresorcinol and caffeic acid shared the collagenase binding sites (Fig. 3A).

236   Four amino acids responsible for caffeic acid attachment included His524, Trp496, His527, and

237   Trp539 (Fig. 3B). His524 and Trp496 interacted caffeic acid by hydrogen bonds through

238   carboxylic and phenolic hydroxyl group(s). His527 and Trp539 bonded to the phenolic ring by

239   π-π stacking. Other amino acids within the enzyme pocket contributed their binding through Van

240   der Waals force (Fig. 3C). Interactions between the collagenase and the bisresorcinol were

241   shown in the Fig. 3D and E, involving Trp496 and Trp539 amino acids that donated π-electrons

242   to bond to the phenolic ring of the bisresorcinol. The presence of hydrogen bonds between the

243   hydroxyl groups of the bisresorcinol and amino acids Asp601 and Ser602 was observed.

244   Moreover, the Zn atom in the enzyme active site might be coordinated to both the bisresorcinol

245   and caffeic acid.

246   The crystal structure of pig elastase (PDB ID 1BRU) was adopted to determine binding

247   behaviors to elastase enzyme of the bisresorcinol and other known inhibitors, including ursolic

248   acid. Results were shown in Fig. 4 and Table S2 (supplement document). The binding energy of

249   all test compounds ranged between -5.62 and -8.94 kcal mol^{-1} and that of -5.69 kcal mol^{-1} was

250   calculated for the bisresorcinol.

251   There was similarity in binding to the elastase of the bisresorcinol and ursolic acid (Fig.

252   4A). Regarding ursolic acid, hydrogen bonding was proposed for a cyclic aliphatic hydroxyl

253   group and Ser96, as well as a carboxylic group and Asn192 (Fig. 4B and C). Interestingly,

254   structural folding of the bisresorcinol was presumed. This might facilitate interactions between

255   phenolic hydroxyl groups of the compound and amino acids like Asn147, Ser190, Phe215, and

256   Ser217 through hydrogen bonding (Fig. 4D and E).

257   To investigate binding affinity to tyrosinase of compounds, the crystal structure of

258   mushroom tyrosinase (PDB ID 2Y9X) was applied. Results were displayed in Fig. 5 and Table

259   S3 (supplement information), indicating that the binding energy of the bisresorcinol was -6.57

260   kcal mol^{-1}, being in a range of -4.63 to -8.12 kcal mol^{-1} for other known inhibitors. In contrast,

261   all known substrates were tightly bound to the tyrosinase according to an enormous decrease of

262   the binding energy to a range from -15.46 and -23.94 kcal mol^{-1}.

263   The coordinate covalent bonds between metal ions and β-arbutin or the bisresorcinol at

264   the tyrosinase active site likely occurred. However, copper ions (Cu^{2+}) were replaced by zinc

265   ions (Zn^{2+}) in the AutodockTool, because the force field for Cu^{2+} is unavailable and Cu^{2+} and

266   Zn^{2+} ions are quite identical in charges and sizes (Santos-Martins *et al.,* 2014). For β-arbutin, one

267   zinc ion might covalently bond to the phenolic hydroxyl group, and another zinc ion interacted

268   with the phenol ring through π-cation bond with His259 and His263 residues (Fig. 5B and C). In

269   addition, the amino acids, such as Asn260, Ser282, and Val283, are linked to its hydroxyl groups

270   by hydrogen bonding. In view of the bisresorcinol, the phenolic hydroxyl group formed

271   hydrogen bonds with Met280, Ala 246, and Glu239. The π-π stacked interaction between the

272   phenol ring and His263, and the π-cation attraction between another phenol ring and Arg321

273   were distinctly observed.

274   In summary, molecular interactions and binding affinity between the bisresorcinol and

275   collagenase, elastase, or tyrosinase were tabulated in Table 2.

276

Discussion

278   Curcuminoid, a phenolic compound from *Curcuma longa* L., has been included in various

279   cosmetic products as an antioxidant for anti-aging property (Gopinath & Karthikeyan, 2018).

280   Since phenolic hydroxy determinants were existent, the bisresorcinol from *H. terminalis*'s trunk

281   was anticipated to harbor anti-aging activity accordingly (Fig. 1). In the recent *in vitro* inhibitory

282   assays, the bisresorcinol was found to dominantly inhibit elastase and tyrosinase activities rather

283   than collagenase counterpart (Fig. 2). Accordingly, *in silico* docking experiments were

284   performed to ascertain binding affinity of the bisresorcinol relevant to these aging enzymes.

285   Interactions regarding π-electrons and hydrogen bonds were assumed to be key determinants for

286   its bindings. Moreover, hydrophobic interactions that occurred between phenolic hydroxyl

287   groups and amino acid residues at/nearby the enzyme active sites might be contributors for loss

288   of enzyme functions, consisting with the previous literatures (Medvidović-Kosanović *et al.,*

289   2010; Pientaweeratch, Panapisal & Tansirikongkol, 2016). Herein, binding characteristics of the

290   bisresorcinol to each enzyme were distinctly explained based on structural comparison

291   corresponding to a specific inhibitor. Inhibition of clostridial collagenase by caffeic acid, EGCG,

292   quercetin, and catechin has been documented (Szewczyk et al., 2020; Pluemsamran *et al.,* 2012;

293   Hong *et al.,* 2014). Similar to other known inhibitors, the hydroxy phenol groups of the

294   bisresorcinol were suggested to interact with key amino acids of the collagenase binding site

295   through π-π interaction and hydrogen bonding. Interestingly, the long flexible structure of

296   bisresorcinol had a capability to fold or elongate. Thus, when elongated, the unbound phenol ring

297   on the other side could bind to amino acid residues at the active site, resulting in increased

298   binding strength. By this way, inhibitory potential of the bisresorcinol on collagenase activity

299   was proposed (Fig. 6).

300   In agreement with a previous study (Huang *et al.,* 2013), binding to elastase enzyme of

301   both the bisresorcinol and known inhibitors, such as procyanidin, quercetin and ursolic acid,

302   were identical, involving hydrogen bond formation. Moreover, interactions between the

303   bisresorcinol and amino acids apart from the enzyme pocket were speculated to mediate the

304   unfolded phenol ring of the substance (Fig. 7).

305   In view of tyrosinase inhibitory activity, inhibitors like kojic acid, rutin, and L-mimosine,

306   have been apparent to competitively bind to tyrosinase enzyme with L-tyrosine, leading to

307   inhibition of melanin synthesis (Channar *et al.,* 2018; Nguyen & Tawata, 2015; Si *et al.,* 2012).

308   In Fig. 8, the π-π interactions between any test compound and histidine residues of the copper

309   active site of tyrosinase were suggested. In agreement with a previous research, this particularly

310   provided an explanation for other antagonistic effects on tyrosinase activity of such compounds

311   (Lai *et al.,* 2017). In fact, the phenolic skeleton in structures has been implicated in designing

312   derivatives of indanone (Jung et al., 2019) and thiazolyl resorcinol (Mann et al., 2018),

313   supporting the possibility of using the bisresorcinol as an antagonist of tyrosinase enzyme.

314

315 **Conclusion**

316 The bisresorcinol might serve as a competitive inhibitor for collagenase, elastase, and tyrosinase

317 with comparable modes of binding compared to known inhibitors. However, the long and

318 flexible structure of the bisresorcinol was interesting in that additional interactions towards an

319 unbound phenol ring to neighboring amino acids of the enzymes might be apparent. This finding

320 was firstly reported and might give an idea for development of new cosmetic products containing

321 the bisresorcinol for anti-aging and whitening effects. Nevertheless, there were further needs to

322 examine its potency *in vivo* and by clinical trials.

323

324 **Acknowledgements**

325 The authors sincerely thank to other research facility providers, such as the Graduate School at

326 Prince of Songkla University; Drug Delivery System Excellence Center, Faculty of

327 Pharmaceutical Sciences, Prince of Songkla University; the Graduate School of Biomedical and

328 Health Sciences (Pharmaceutical Sciences), Hiroshima University, Hiroshima, Japan; and

329 Department of Biomedical Sciences and Biomedical Engineering, Faculty of Medicine, Prince of

330 Songkla University, Thailand.

331

332 **References**

333 **Abhijit S, Manjushree D. 2010.** Anti-hyaluronidase, anti-elastase activity of *Garcinia indica*.

334   *International Journal of Botany* **6(3)**:299-303 DOI 10.3923/ijb.2010.299.303.

335 **BIOVIA. 2020.** Discovery studio. San Diego: Dassault Systèmes.

336 **Channar PA, Saeed A, Larik FA, Batool B, Kalsoom S, Hasan MM, Ashraf Z. 2018.**

337   Synthesis of aryl pyrazole via Suzuki coupling reaction, *in vitro* mushroom tyrosinase

338   enzyme inhibition assay and *in silico* comparative molecular docking analysis with kojic

339   acid. *Bioorganic Chemistry* **79**:293-300 DOI 10.1016/j.bioorg.2018.04.026.

340 **Chaturvedula VP, Schilling JK, Miller JS, Andriantsiferana R, Rasamison VE, Kingston**

341   **DG. 2002.** New cytotoxic bis 5-alkylresorcinol derivatives from the leaves of *Oncostemon*

342   *bojerianum* from the Madagascar rainforest. *Journal of natural products* **65(11)**:1627-1632

343   DOI 10.1021/np0201568.

344 **Dobos G, Lichterfeld A, Blume-Peytavi U, Kottner J. 2015.** Evaluation of skin ageing: a

345   systematic review of clinical scales. *British Journal of Dermatology* **172(5)**:1249-1261 DOI

346   10.1111/bjd.13509.

347 **European Commission, Scientific Committee on Consumer Safety. 2010.** Opinion on

348   resorcinol, SCCS/1270/09. Available at: https://ec.europa.eu/health/scientific_

349   committees/consumer_safety/docs/sccs_o_015.pdf **(accessed 19 February 2021)**

350 **Giang PM, Nga NT, Van Trung B, Anh DH, Viet PH. 2019.** Evaluation of the antioxidant,

351   hepatoprotective, and anti-inflammatory activities of bisresorcinol isolated from the trunk of

352   *Heliciopsis terminalis*. *Pharmaceutical Chemistry Journal* **53(7)**:628-634 DOI

353   10.1007/s11094-019-02051-7.

354 **Gopinath H, Karthikeyan K. 2018.** Turmeric: a condiment, cosmetic and cure. *Indian Journal*

355   *of Dermatology Venereology and Leprology* **84(1)**:16 DOI 10.4103/ijdvl.IJDVL_1143_16.

356 **Hong YH, Jung EY, Noh DO, Suh HJ. 2014**. Physiological effects of formulation containing

357   tannase-converted green tea extract on skin care: physical stability, collagenase, elastase, and

358   tyrosinase activities. *Integrative medicine research* **3(1)**:25-33 DOI

359   10.1016/j.imr.2013.12.003.

360   **Huang Y, Chen L, Feng L, Guo F, Li Y. 2013.** Characterization of total phenolic constituents

361   from the stems of *Spatholobus suberectus* using LC-DAD-MS^n and their inhibitory effect on

362   human neutrophil elastase activity. *Molecules* **18(7)**:7549-7556 DOI

363   10.3390/molecules18077549.

364   **Humphrey W, Dalke A, Schulten K. 1996.** VMD – Visual Molecular Dynamics. *Journal of*

365   *Molecular Graphics* **14(1)**:33-38 DOI 10.1016/0263-7855(96)00018-5.

366   **Jewboonchu J, Saetang J, Saeloh D, Siriyong T, Rungrotmongkol T, Voravuthikunchai SP,**

367   **Tipmanee V. 2020.** Atomistic insight and modeled elucidation of conessine towards

368   *Pseudomonas aeruginosa* efflux pump. *Journal of Biomolecular Structure and Dynamics*

369   **Oct 7**:1-10 DOI 10.1080/07391102.2020.1828169.

370   **Jiratchayamaethasakul C, Ding Y, Hwang O, Im ST, Jang Y, Myung SW, Lee JM, Kim**

371   **HS, Ko SC, Lee SH. 2020.** *In vitro* screening of elastase, collagenase, hyaluronidase, and

372   tyrosinase inhibitory and antioxidant activities of 22 halophyte plant extracts for novel

373   cosmeceuticals. *Fisheries and Aquatic Sciences* **23(1)**:1-9 DOI 10.1186/s41240-020-00149-

374   8.

375   **Jung HJ, Noh SG, Park Y, Kang D, Chun P, Chung HY, Moon HR. 2019.** *In vitro* and *in*

376   *silico* insights into tyrosinase inhibitors with (E)-benzylidene-1-indanone derivatives.

377   *Computational and structural biotechnology journal* **17**:1255-1264. DOI

378   10.1016/j.csbj.2019.07.017.

379 **Lai X, Wichers HJ, Soler-Lopez M, Dijkstra BW. 2017.** Structure of human tyrosinase related

380   protein 1 reveals a binuclear zinc active site important for melanogenesis. *Angewandte*

381   *Chemie International Edition* **56(33)**:9812-9815 DOI 10.1002/anie.201704616.

382 **Mann T, Scherner C, Röhm KH, Kolbe L. 2018.** Structure-activity relationships of thiazolyl

383   resorcinols, potent and selective inhibitors of human tyrosinase. *International journal of*

384   *molecular sciences* **19(3)**:690 DOI 10.3390/ijms19030690.

385 **Medvidović-Kosanović M, Šeruga M, Jakobek L, Novak I. 2010.** Electrochemical and

386   antioxidant properties of (+)-catechin, quercetin and rutin. *Croatica chemica acta* **83(2)**:197-

387   207

388 **Nguyen BCQ, Tawata S. 2015.** Mimosine dipeptide enantiomsers: improved inhibitors against

389   melanogenesis and cyclooxygenase. *Molecules* **20(8)**:14334-14347 DOI

390   10.3390/molecules200814334.

391 **Pientaweeratch S, Panapisal V, Tansirikongkol A. 2016.** Antioxidant, anti-collagenase and

392   anti-elastase activities of *Phyllanthus emblica*, *Manilkara zapota* and silymarin: an *in vitro*

393   comparative study for anti-aging applications. *Pharmaceutical biology* **54(9)**:1865-1872.

394   DOI 10.3109/13880209.2015.1133658.

395 **Pluemsamran T, Onkoksoong T, Panich U. 2012.** Caffeic acid and ferulic acid inhibit UVA-

396   induced matrix metalloproteinase-1 through regulation of antioxidant defense system in

397   keratinocyte HaCaT cells. *Photochem. Photobiol* **88**:961–968 DOI 10.1111/j.1751-

398   1097.2012.01118.x.

399 **Saeloh D, Wenzel M, Rungrotmongkol, T, Hamoen, LW, Tipmanee V, Voravuthikunchai**

400   **SP. 2017**. Effects of rhodomyrtone on Gram-positive bacterial tubulin homologue FtsZ.

401   *PeerJ* **5**:e2962 DOI doi: 10.7717/peerj.2962.

402   **Santos-Martins D, Forli S, Ramos MJ, Olson AJ. 2014.** AutoDock4$_{Zn}$: an improved AutoDock

403   force field for small-molecule docking to zinc metalloproteins. *Journal of chemical*

404   *information and modeling* **54(8)**:2371-2379 DOI 10.1021/ci500209e.

405   **Selvaraj S, Krishnaswamy S, Devashya V, Sethuraman S, Krishnan UM. 2014.** Flavonoid–

406   metal ion complexes: a novel class of therapeutic agents. *Medicinal Research Reviews*

407   **34(4)**:677-702 DOI 10.1002/med.21301.

408   **Sherratt MJ, Hopkinson L, Naven M, Hibbert SA, Ozols M, Eckersley A, Newton VL, Bell**

409   **M, Meng QJ. 2019**. Circadian rhythms in skin and other elastic tissues. *Matrix Biology*

410   **84**:97-110 DOI 10.1016/j.matbio.2019.08.004.

411   **Si YX, Yin S J, Oh S, Wang ZJ, Ye S, Yan L, Yang JM, Park YD, Lee J, Qian GY. 2012.**

412   An integrated study of tyrosinase inhibition by rutin: progress using a computational

413   simulation. *Journal of Biomolecular Structure and Dynamics* **29(5)**:999-1012 DOI

414   10.1080/073911012010525028.

415   **Szewczyk K, Miazga-Karska M, Pietrzak W, Komsta Ł, Krzemińska B, Grzywa-Celińska**

416   **A. 2020**. Phenolic composition and skin-related properties of the aerial parts extract of

417   different *Hemerocallis cultivars*. *Antioxidants* **9(8)**:690 DOI 10.3390/antiox9080690.

418   **Tanawattanasuntorn T, Thongpanchang T, Rungrotmongkol T, Hanpaibool C, Graidist P,**

419   **Tipmanee V. 2020.** (−)-Kusunokinin as a potential aldose reductase inhibitor: equivalency

420   observed via AKR1B1 dynamics simulation. *ACS Omega* **6(1)**:606-614 DOI

421   10.1021/acsomega.0c05102.

422   **Teajaroen W, Phimwapi S, Daduang J, Klaynongsruang S, Tipmanee V, Daduang S. 2020.**

423   A role of newly found auxiliary site in phospholipase A1 from Thai banded tiger wasp

424   (*Vespa affinis*) in its enzymatic enhancement: *in silico* homology modeling and molecular

425   dynamics insights. *Toxins* **12(8)**:510 DOI 10.3390/toxins12080510.

426   **Thring TS, Hili P, Naughton DP. 2009**. Anti-collagenase, anti-elastase and anti-oxidant

427   activities of extracts from 21 plants. *BMC complementary and alternative medicine* **9(1):**1-11

428   DOI 10.1186/1472-6882-9-27.

429   **Widyowati R, Sugimoto S, Yamano Y, Sukardiman, Otsuka H, Matsunami K. 2016**. New

430   isolinariins C, D and E, flavonoid glycosides from *Linaria japonica*. *Chemical and*

431   *Pharmaceutical Bulletin* **64(5)**:517-521 DOI 10.1248/cpb.c16-00073.

Figure 1

Chemical structures of compounds.

(A), Bisresorcinol isolated from *H. terminalis*'s trunk; (B), caffeic acid; (C), ursolic acid; and
(D), β-arbutin.
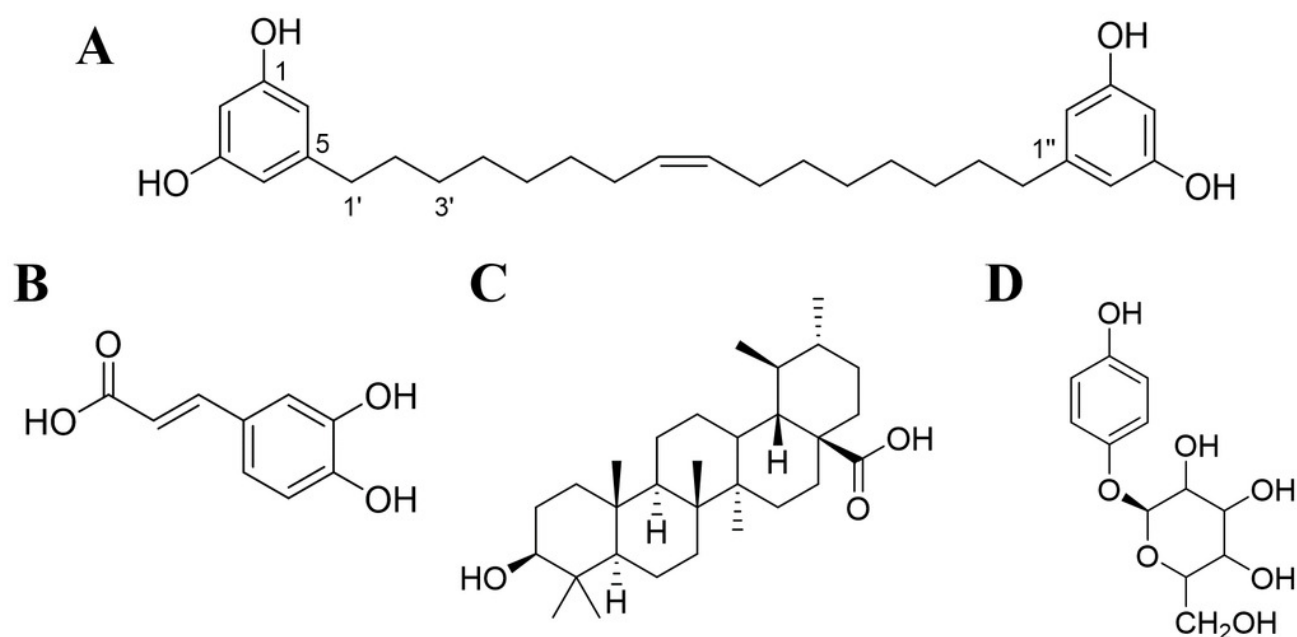
Figure 2

Response of inhibition percentage

Response of % inhibition, evaluated by linear regression analysis and correlation coefficients expressed as R^2 shown in the panels; A, collagenase inhibition in compared to caffeic acid; B, elastase inhibitory activity using ursolic acid as a positive control; and C, tyrosinase inhibitory assay in comparison with β-arbutin

A

R² = 0.9954

R² = 0.9882

% Inhibition

Concentration (μM)

▲ Bisresorcinol   ■ Caffeic acid

B

R² = 0.896

R² = 0.9228

% Inhibition

Concentration (μM)

▲ Bisresorcinol   ■ Ursolic acid

C

R² = 0.9625

R² = 0.9925

% Inhibition

Concentration (μM)

▲ Bisresorcinol   ■ β-arbutin
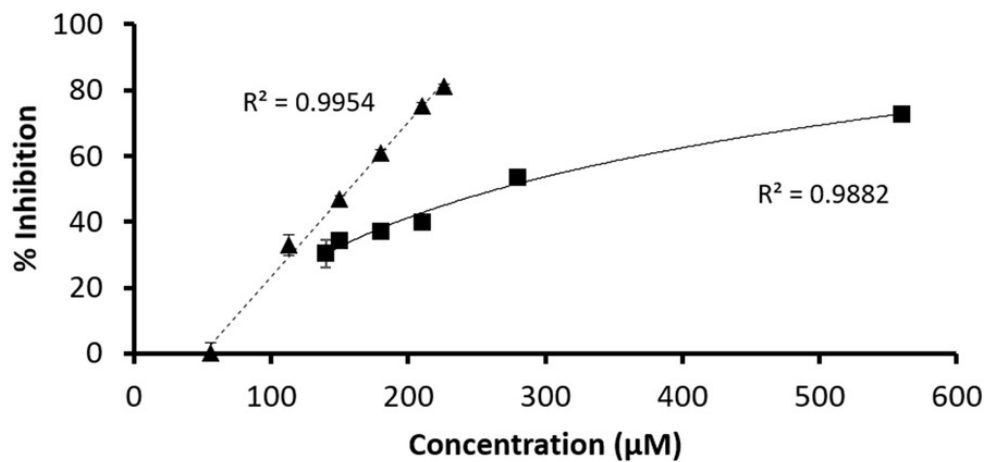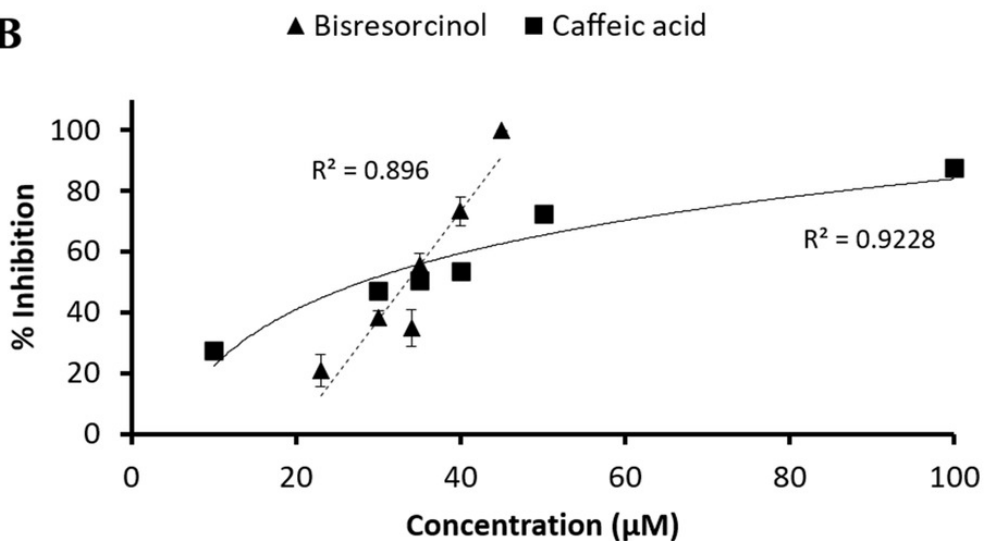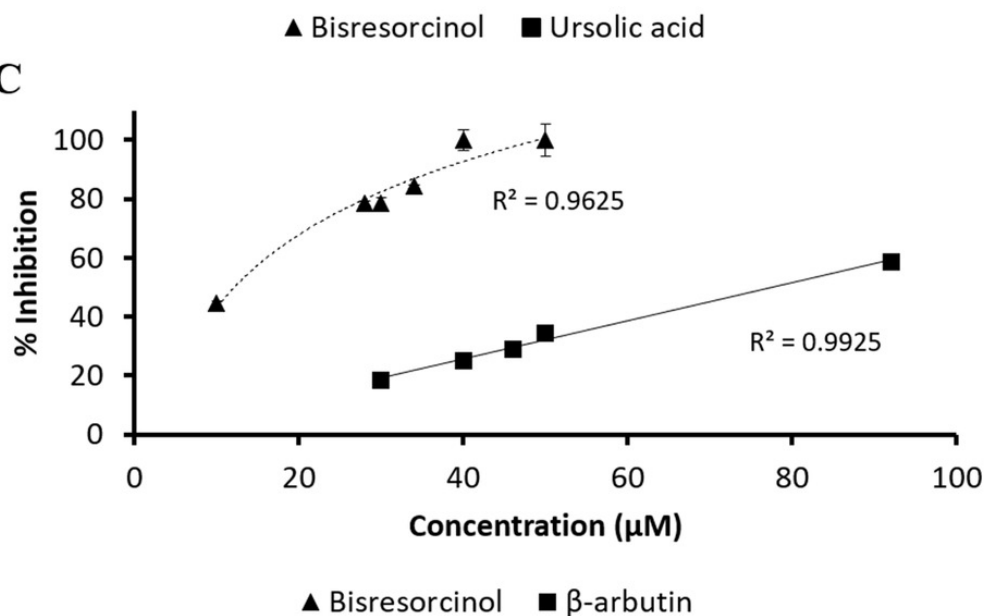
Figure 3

Collagense bound ligands

(A) Molecular docking model of caffeic acid (red) and the bisresorcinol (blue) on the collagenase active site. Ligand interaction diagrams of caffeic acid (B-C) and the bisresorcinol (D-E), involving the π - π stacking, hydrogen bond, and Van der Waals as respectively depicted in pink, green, and grey.
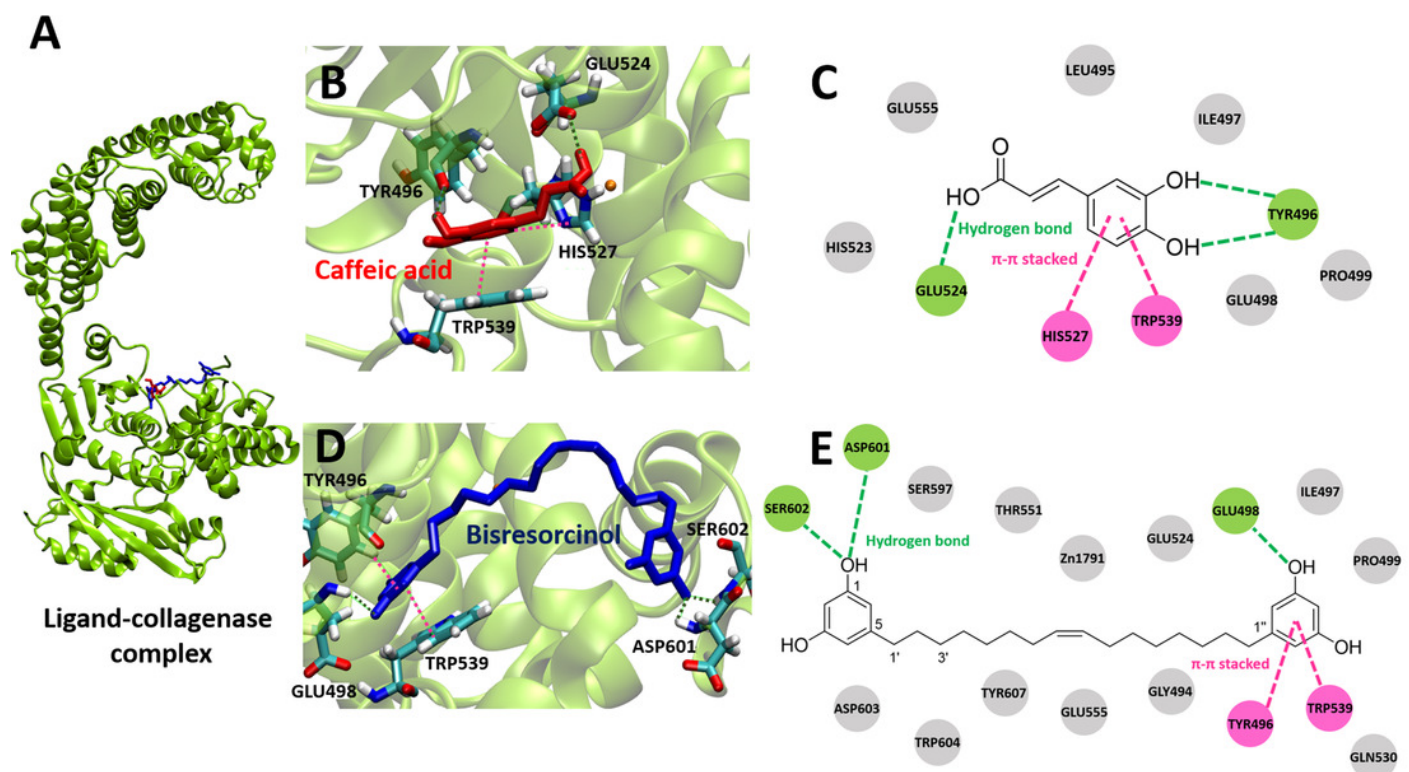
Figure 4

Elastase bound ligands

(A) Binding characteristics of the bisresorcinol (blue) and ursolic acid (red) to the active site of pig elastase; (B-C), Ligand-protein interaction diagrams of ursolic acid (B-C) and the bisresorcinol (D-E); Interactions involved π-π stacking, hydrogen bonds, and Van der Waals force, depicted in pink, green, and grey, respectively.
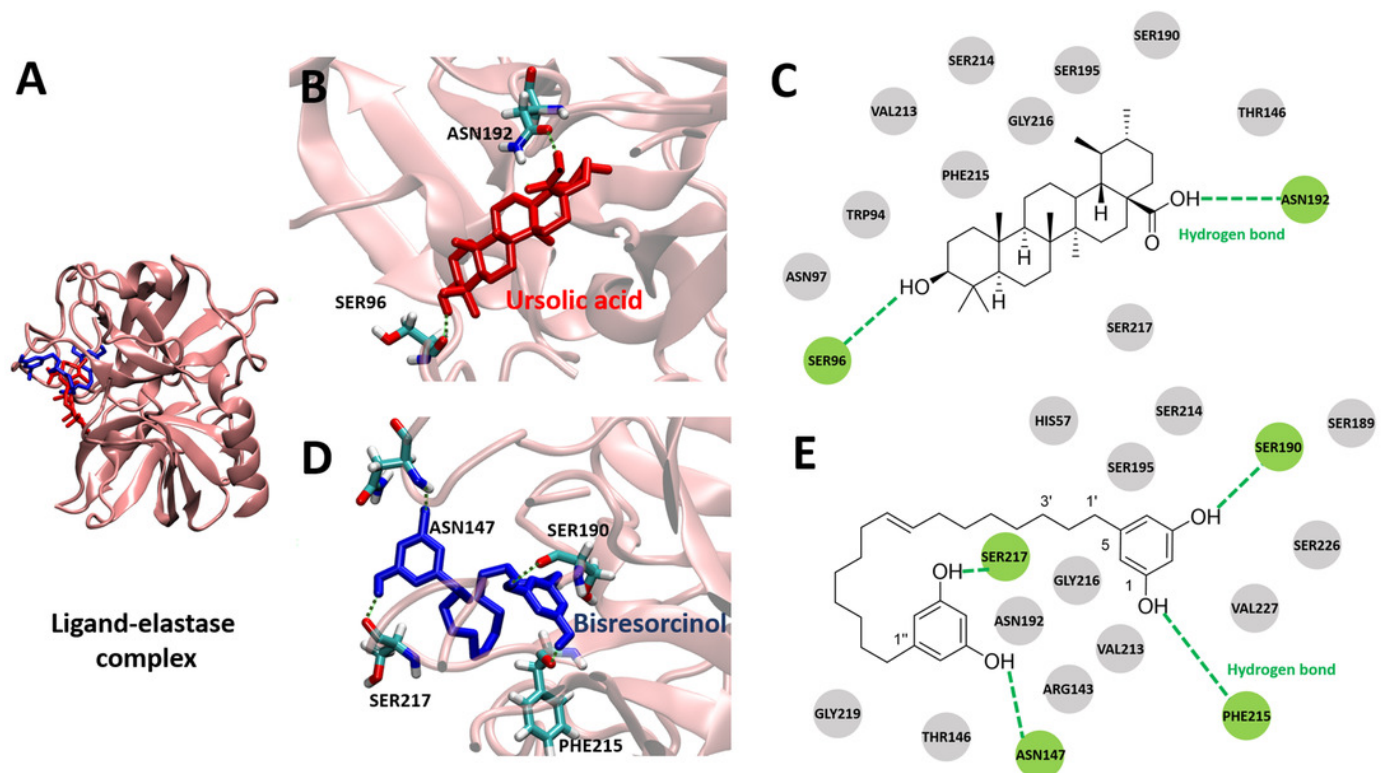
Figure 5

Tyrosinase bound ligands

(A) Molecular docking model of β-arbutin (red) and the bisresorcinol (blue) on the tyrosinase active site. Ligand-protein interaction diagrams of β-arbutin (B-C) and the bisresorcinol (D-E) showed the engagement of π-cation, π-π stacking, hydrogen bonding, and van der waals force, depicted in orange, pink, green, and grey, respectively
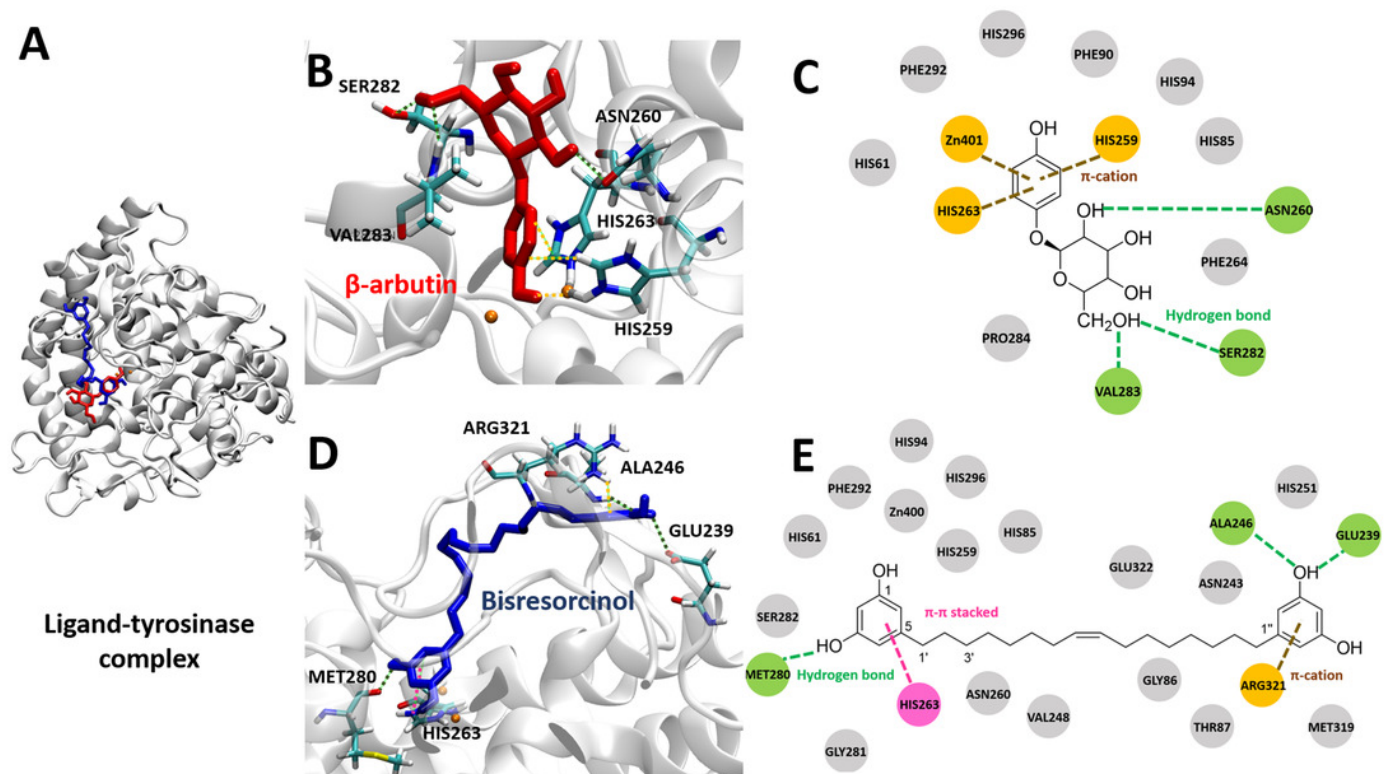
Figure 6

Binding modes of collagenase inhibitors

Binding modes of inhibitors namely caffeic acid, catechin, EGCG, and quercetin, and the bisresorcinol on collagenase enzyme; Symbols: red dash lines, hydrogen bonds; green dash lines, π-interactions.
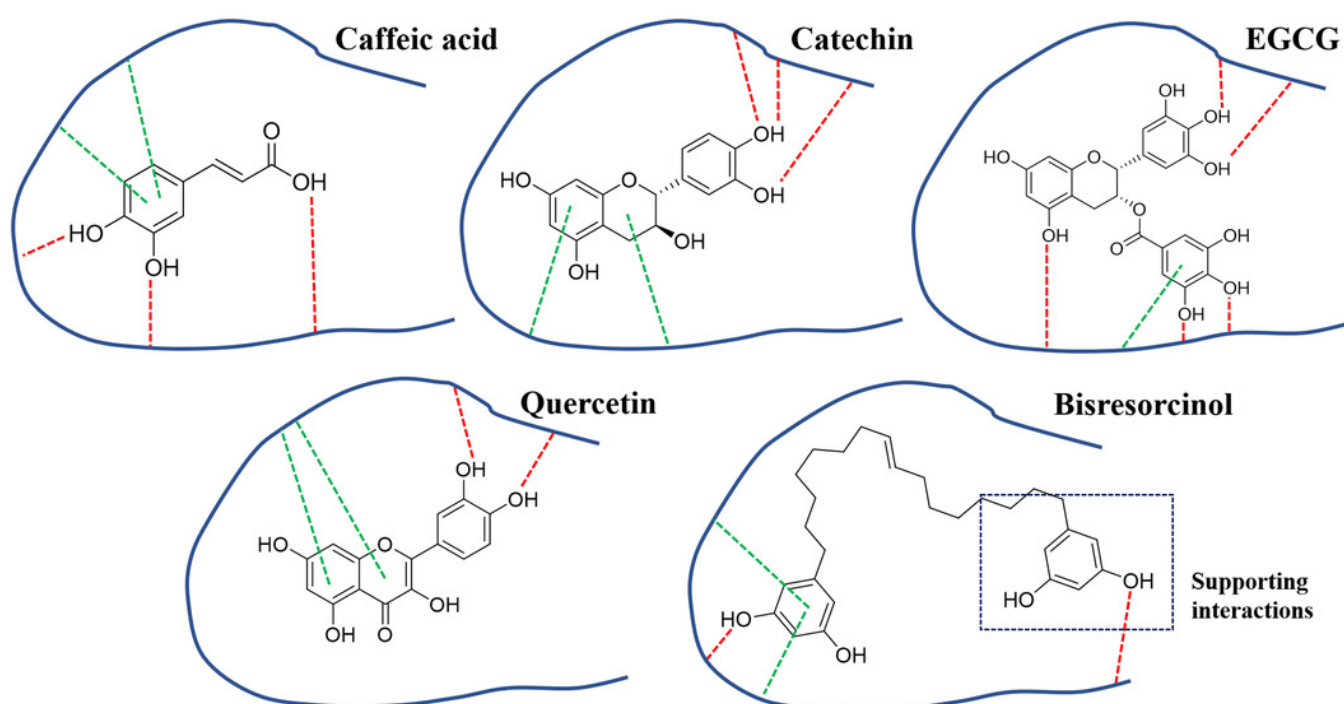
Figure 7

Binding modes of elastase inhibitors

Binding modes of actions of the bisresorcinol and known inhibitors, such as quercetin, procyanidin, and ursolic acid on elastase enzyme; Symbol: red dash lines, hydrogen bonds.
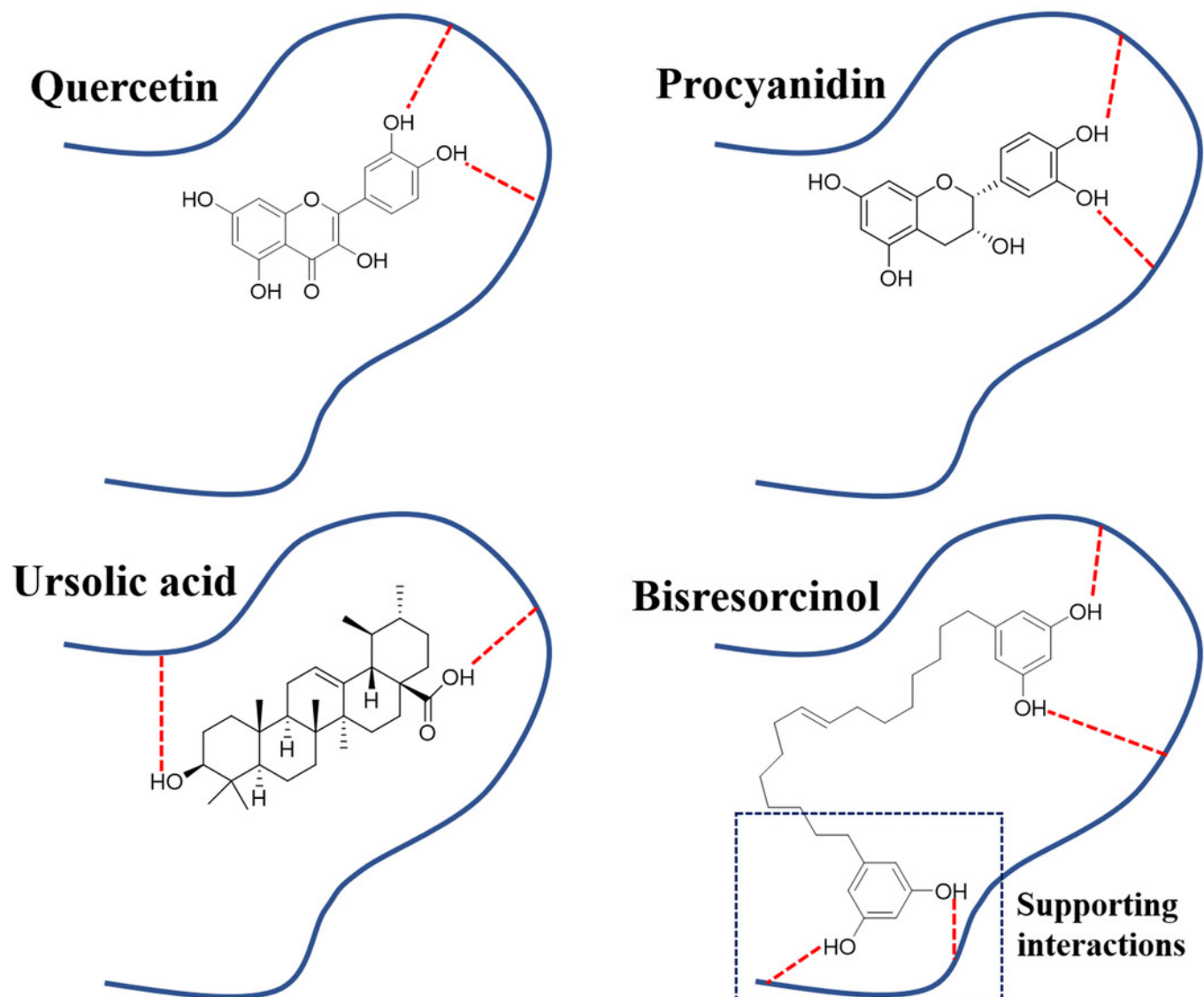
Figure 8

Binding modes of tyrosinase inhibitors

Binding modes of actions of the bisresorcinol and known inhibitors, e.g., kojic acid, L-mimosine, and rutin, on mushroom tyrosinase; Symbols: red dash lines, hydrogen bonds; green dash lines, π-interactions.
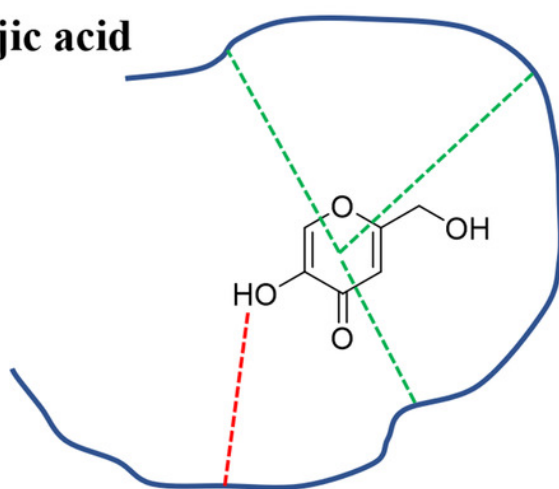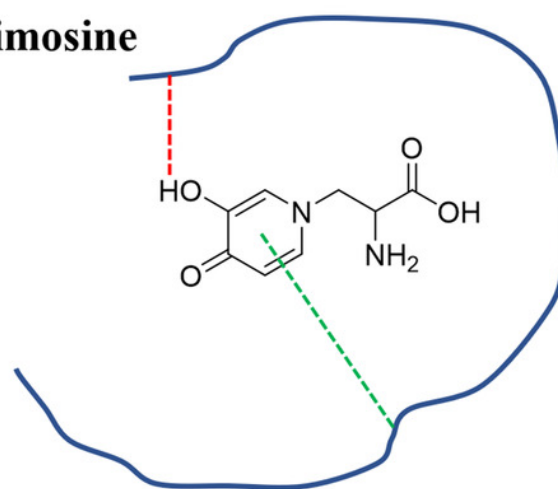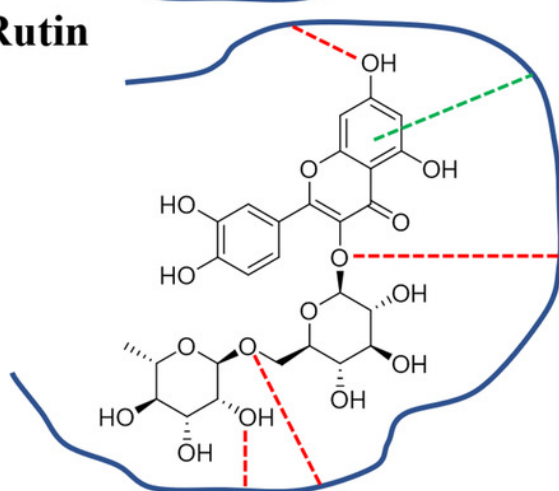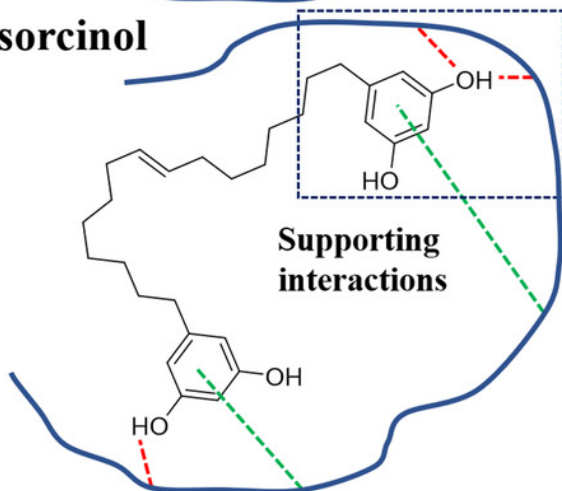
The IC50 values of the bisresorcinal and positive standards for enzymatic inhibitory assays regarding collagenase, elastase, and tyrosinase; *, p < 0.01; **, p < 0.001

—

1 **Table 1** The IC_{50} values of the bisresorcinal and positive standards for enzymatic inhibitory

2 assays regarding collagenase, elastase, and tyrosinase; *, $p < 0.01$; **, $p < 0.001$

Assay	IC_{50} (µmole L^{-1}±SEM)
Collagenase Inhibition	
Bisresorcinol	156.7±2.3 ⎫
Caffeic acid	308.9±13.7 ⎭ *
Elastase Inhibition	
Bisresorcinal	33.2±1.1
Ursolic acid	34.3±0.6
Tyrosinase Inhibition	
Bisresorcinol	22.6±1.3 ⎫
β-Arbutin	78.5±3.1 ⎭ **

Table 2

Binding energy and amino acid residues that participated in the binding

1 **Table 2** Binding energy and amino acid residues that participated in the binding

Ligand	Binding energy (kcal/mol)	Binding residue
Collagenase inhibitor		
Caffeic acid	-6.86	**Glu524, Tyr496,** His527, Trp539, Glu498, Glu555, His523, Ile497, Leu495, Pro499
Bisresorcinol	-5.89	**Asp601, Glu498, Ser602,** Tyr496, Trp539, Asp603, Gln530, Glu524, Glu555, Gly494, Ile497, Pro499, Thr551, Trp604, Tyr607, Ser597, Zn1791
Elastase inhibitor		
Ursolic acid	-8.94	**Asn192, Ser96,** Asn97, Gly216, Phe215, Ser190, Ser195, Ser214, Ser217, Thr146, Trp94, Val213
Bisresorcinol	-5.69	**Asn147, Phe215, Ser190, Ser217,** Asn192, Arg143, Gly216, Gly219, His57, Ser189, Ser195, Ser214, Ser226 Thr146, Val213, Val227
Tyrosinase inhibitor		
β-arbutin	-5.52	*His259, His263, Zn401* **Asn260, Ser282, Val283,** His61, His85, His94, His296, Phe90, Phe264, Phe292, Pro284
Bisresorcinol	-6.57	*Arg321,* **Ala246, Glu239, Met280,** His263, Asn243, Asn260, Glu322, Gly86, Gly281, His61, His85, His94, His251, His259, His296, Met319, Phe292, Ser282, Thr87, Val248, Zn400

2 Note: π-cation, π - π stacking, and hydrogen bonds were depicted in italic, underline, and bold,
3 respectively. The normal letter represented amino acids containing and Van der Waals interactions
4 with the compound.